THE ASTROPHYSICAL JOURNAL, 213:438–447, 1977 April 15

SPECTROSCOPIC STUDIES OF O-TYPE STARS. VII. ROTATIONAL VELOCITIES $V \sin i$ AND EVIDENCE FOR MACROTURBULENT MOTIONS

PETER S. CONTI* AND DENNIS EBBETS
Joint Institute for Laboratory Astrophysics, University of Colorado and National Bureau of Standards, and Department of Astrogeophysics, University of Colorado
Received 1976 July 30; revised 1976 October 7

ABSTRACT

Rotational velocities are derived from coudé spectrograms of 205 O-type stars in the northern and southern hemispheres. The velocity distribution for main-sequence stars is bimodal, containing a slow group with a $V \sin i$ peak near 100 km s^{-1} and a fast group with a $V \sin i$ peak near 300 km s^{-1}. The distribution of type III giants shows fewer of the high-velocity stars, and the type I supergiants are all distributed around a single peak near $V \sin i = 100$ km s^{-1}. A number of Oe stars are found in the rapidly rotating group, by analogy with Be stars. The peak of the velocity distribution of the giants and supergiants does not shift as much to slower velocities as would have been expected from the peak for the main-sequence stars and stellar evolution leading to an increasing radius, with angular momentum conserved in shells. The detailed shapes of the distributions do not agree well with a purely rotational interpretation of the broadening, especially for the giants and supergiants. These facts, and the absence of any very sharp-lined supergiants, suggest that an additional parameter—turbulence—is probably necessary in evolved O-type stars.

Subject headings: stars: early-type — stars: rotation — turbulence

I. INTRODUCTION

One of the most notable characteristics of the visible spectra of the O-type stars is the absence of sharp absorption lines. Lines of various elements, including H, He I, He II, C III, N III, O III, and Si IV, can be identified; but they are usually quite broad and shallow. When equivalent widths are measured, principally He I λ4471 and He II λ4541, the spectra can be arranged in an orderly sequence of spectral types in which the widths change in a very systematic way (Conti and Alschuler 1971, hereafter Paper I). Furthermore, the measured line strengths agree quite well with those predicted by non-LTE model atmospheres (Auer and Mihalas 1972) characterized by effective temperatures in the range 30,000 to 50,000 K, and surface gravities between $\log g = 3.3$ and 4.0 (Conti 1973). The profiles of the lines, however, appear to be broader than those computed for hydrostatic plane-parallel atmospheres.

The two most commonly discussed mechanisms which may account for the broadened profiles are stellar rotation and atmospheric motion of some sort: micro- or macroturbulence. Attempts to compute the shapes of narrow line profiles broadened by rotation indeed predict profiles very much like those actually observed. However, there are reasons to suspect that rotation may not be the sole culprit in the O stars. The most disturbing fact is the lack of clear evidence of an O star with sharp lines, as would be expected from a rotating star seen pole-on. Presumably, out of a large enough sample of stars, we should see at least a few nearly pole-on, but we still observe considerable broadening in all of them. This additional broadening could be due to large-scale atmospheric motions occurring everywhere on the stellar surface. Such motions seem rather plausible, for the more luminous stars especially, where high luminosity and larger radius make the balance between radiation pressure and gravity more precarious. Rosendahl (1970) has shown, in fact, that among B- and A-type supergiants, macroturbulence is an important contributor to overall line width.

Early attempts by Slettebak (1956) to estimate what a line broadened by macroturbulence would look like also produced profiles that appear quite similar to those observed. It thus seems difficult to decide which mechanism is the dominant cause of the observed profiles. The purpose of this paper is to measure observed profiles in a large number of O and Of stars and see *what rotational velocities* ($V \sin i$) *are implied if rotation is the sole source of broadening*. The more significant question of the contribution of turbulence to the line broadening is at present being investigated in detail for a few stars and will be reported upon subsequently. In § II, we discuss the basis on which theoretical profiles were constructed. We present the observational data in § III. For a set of standard stars, line profiles are derived to compare with the theoretical ones. For most stars, visual eye estimates of $V \sin i$ are then given from comparison with the standards. In § IV, we analyze the $V \sin i$ distribution for the O stars and discuss the results.

* Also Department of Physics and Astrophysics, University of Colorado, and Visiting Astronomer, Cerro Tololo Inter-American Observatory, operated by AURA, Inc., under contract with the National Science Foundation.

II. THEORY

Historically, the determination of $V \sin i$ has been approached in several similar ways. In the first method, the sample of stars to be measured is divided into groups, each having similar spectral types and luminosities. The sharpest-lined star in each group is assumed to be not influenced by rotation, and its lines are used as zero-velocity profiles. These profiles are then broadened mathematically with various degrees of sophistication, and an assortment of other effects—continuum limb darkening, gravity darkening, differential rotation, electron scattering, etc.—sometimes approximated.

Two significant problems detract from the usefulness of this approach for the O stars. The first problem, as discussed above, is that no O stars have really sharp lines. Two of the sharpest are 10 Lac and HD 57682, both of which have been used. However, even their profiles do not perfectly match zero-velocity models, and probably have some additional broadening. The second difficulty is that both these stars are about the same spectral type and luminosity class (O8 or O9, V or III, according to various authors). Consequently, even if these stars are indeed nonrotators, results derived from them would be reliable only for other stars of similar spectral types. As one proceeds to earlier spectral types or brighter luminosity classes, both the relative strengths and intrinsic profiles of the lines used for measurement change drastically. If these intrinsic changes are ignored, serious errors may result in rotational velocities inferred from measured profiles.

A second, more modern approach starts with theoretical profiles computed from good model atmosphere calculations. The most sophisticated calculations begin with *intensity* profiles, divide the apparent stellar disk into a large number of small areas, Doppler shift the profile by an amount determined by the projected velocity of that area, *then* sum over the disk to derive the resulting flux profile. In this way, the center-to-limb variations of both the line strength and the profile are explicitly accounted for. This can be done for those spectral types and luminosity classes for which one has available intensity profiles, and for sufficient velocities to build a large homogeneous grid of broadened profiles. This was the approach taken by Stoeckley and Mihalas (1973) for lines represented mostly in B-type stars.

The approach taken in the present paper is really a compromise between these two methods. In order to derive a grid of results to adequately represent spectral types O9.5 to O5, and luminosity classes V, III, and I, it was necessary to begin with theoretical profiles. Since Auer and Mihalas (1972) did not provide intensity profiles, we began with their calculated *flux* profiles (of a nonrotating star) and broadened them, using a computer program. The program is essentially a digital version of the usual technique of dividing a uniform, circular stellar disk into a number of strips, finding the velocity of each strip, shifting the profile by that velocity, scaling by the fractional area of the strip, then summing over the disk. The main difference is that this method will give slightly too much weight to contributions from very near the limb, since the flux profile is stronger than an intensity profile would be. Consequently, the highest velocities will be expected to influence the final profile a bit too much, making it slightly shallower and wider. It will be shown that this effect did indeed show up, but only at the highest velocities, and even then only slightly.

Since no one spectral line is very suitable over the entire range of stars to be measured, it was decided to model four lines and use as many of these as possible in the final velocity determination. The lines used were Hγ λ4340, He I λ4388 and 4471, and He II λ4541. The strengths and profiles of these lines change noticeably over the spectral type grid, but at least one is always intrinsically narrow and symmetrical. The nature of the changes is the following. The hydrogen line, Hγ, weakens going from O9 to O5, but not drastically. However, on the main sequence, Hγ has very pronounced wings, due to Stark broadening. The line becomes much narrower at higher luminosities (lower gravities); He I λ4388 is strong and symmetrical at O9, but becomes very weak and is difficult to measure earlier than O7. He I λ4471 also becomes weaker at higher temperatures, and it too is most useful near O9. This line has a forbidden component at λ4470, which is strong enough at type O9 V to produce a noticeable asymmetry in the blue wing. This component is produced by a quadratic Stark effect, and weakens very rapidly with increasing luminosity and temperature. He II λ4541 is very weak at O9, but strengthens rapidly, and is quite strong earlier than O7. Being a hydrogenic ion, He II is Stark affected, and has broad wings on the main sequence, but is narrow and symmetric in giants and supergiants.

In order to test how well the computer program worked, two spectral lines were broadened by several velocities, and the resulting profiles were compared to other results for the same lines. Flux profiles of the two He I lines λ4026 and λ4471 were taken from non-LTE model atmospheres with $T_{\text{eff}} = 27{,}500$ K and $\log g = 4.0$ (Stoeckley and Mihalas 1973). Velocities of 10, 25, 50, 100, 150, 200, 300, and 400 km s^{-1} were used, and the resulting profiles plotted (Fig. 1). The corresponding rotational broadened profiles given by Stoeckley and Mihalas were plotted on the same axes to allow easy comparison. The profiles are absolutely indistinguishable for velocities below 200 km s^{-1}. At higher velocities, our profiles have very slightly shallower cores and deeper wings, but even at 400 km s^{-1} the difference is only about 2% of the continuum.

Flux profiles for the four lines from non-LTE model atmospheres of Auer and Mihalas (1972) were chosen to represent spectral types O9.5, O8.5, and O6.5 ($T_{\text{eff}} = 30{,}000$, 35,000, and 40,000 K), and luminosity classes I and V ($\log g = 3.3$, 4.0). Each line was broadened by several velocities, the maximum being 300 km s^{-1}. The profiles were plotted, the full width at half-central intensity was measured, and its relationship to velocity was plotted. The plots for luminosity

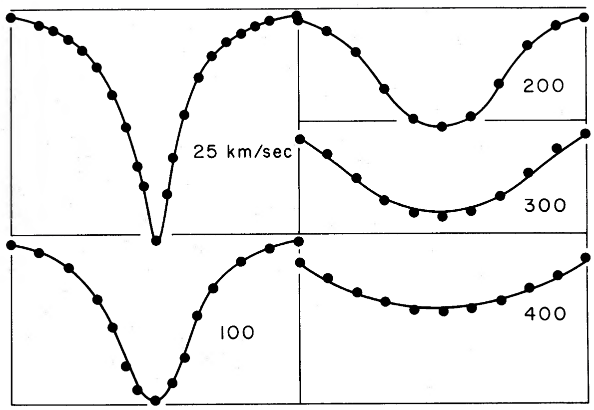

FIG. 1.—Comparison of rotationally broadened profiles computed by the program used in the present work (*solid line*), and that used by Stoeckley and Mihalas 1973 (*dots*). The zero-velocity profile was He I 4026 for a plane-parallel atmosphere with $T_{eff} = 27{,}500$ K and $\log g = 4.0$. The differences at high velocities are due to the explicit treatment of limb darkening used by Stoeckley and Mihalas, as explained in the text.

class III were produced by linear interpolation, point by point, between those for classes I and V. Intermediate spectral types were estimated visually on the graphs.

III. REDUCTION OF OBSERVATIONAL MATERIAL

The observed line profiles were obtained from the same set of 16 Å mm^{-1} Lick coudé plates previously described in Paper I. In addition, we had available a number of 18 Å mm^{-1} coudé spectrograms of southern stars obtained at the 60 inch (1.5 m) telescope of the Cerro Tololo Observatory. We first chose a group of 37 (northern) stars to be standard velocity O stars. We attempted to include as wide a range of velocities and spectral types as possible as well as all of Slettebak's (1956) standards, avoiding where possible known double-lined spectroscopic binaries. The selected stars were then analyzed in detail as follows.

Sections of the spectra spanning the four lines, along with the clear plate, the intensity strip calibration pattern, and the wavelength comparison spectrum, were traced on the microdensitometer at the High Altitude Observatory in Boulder. The digital reduction, which was the same for each spectrum, was performed on the University of Colorado CDC 6400 computer and proceeded as follows. An intensity (H & D) calibration curve was constructed at about λ4420 by fitting a quadratic to the relationship between relative intensity and microdensitometer digital output. A quadratic was also fitted to the entire clear tracing, and this function was subtracted, point by point, from the spectrum, while still in density units. The spectrum was then converted to the relative intensity scale, using the H & D function. From the microfilm output of this spectrum, those of the four spectral lines which were present in sufficient strength to be measured were chosen, their positions noted, and segments of clear continuum identified. An attempt was made to choose the same continuum locations for each spectrum, but sometimes other absorption lines, noise, or plate flaws precluded this. A quartic polynomial was fitted to the length of continuum specified, and the entire spectrum was normalized to this fit. The normalized line profiles from ± 10 Å of line center were output on microfilm, and various pieces of information, including the measured equivalent widths, were printed. These equivalent widths were compared with those previously derived from the same plates in Paper I. No systematic differences were found, ensuring that the final output was reliable. No digital smoothing of the data was attempted. The instrumental profile was small on the velocity scales used here.

Hard copies of the profiles were made, and the full widths at half-intensity were measured. Using the spectral types and luminosity classes assigned by Conti and Leep (1974), we chose the appropriate theoretical half-width versus velocity curves. The implied rotational velocity was then derived independently for each line measured.

As might be expected, the measurements derived from several lines of a given star never agreed perfectly. Therefore weights were assigned to each measurement; and the weighted mean and standard deviation were determined. Weights of either 1, 2, or 3 were assigned somewhat subjectively, based on the intrinsic shape and strength of the line, and an opinion of the reliability of the measurement. The weights used are presented in Table 1. The mean rotational velocities and the standard deviations are contained in Table 2.

In Figure 2, the measurements from individual lines are plotted against the weighted mean. The individual measurements from all four lines scatter about the mean, indicating random errors.

Column (5) of Table 2 lists the velocities adopted by Slettebak (1956) from measurements of up to seven lines. Figure 3 is a plot of those 21 stars. At low velocities ($V \sin i < 150$ km s^{-1}) the new values appear to be systematically slower, by perhaps 30 km s^{-1}. The agreement appears to be better, though, at higher velocities. Most of this change can probably be understood in terms of arguments presented earlier, as

TABLE 1

WEIGHTS USED IN THE CALCULATIONS OF THE MEAN ROTATIONAL VELOCITIES OF STANDARD STARS

		V	III	I
O9, O8	Hγ	1	2	3
	4388	3	3	3
	4471	3	3	3
	4541	1	1	1
O7, O6	Hγ	1	2	3
	4388	3	2	2
	4471	3	3	3
	4541	1	2	2
O5, O4	Hγ	1	2	2
	4388	1	1	1
	4471	1	1	1
	4541	1	3	3

Table 2

Standard Velocity O Stars

Star	Spectral Type	V sin i	σ	Slettebak
46202	09V	15	9	
57682	09V	17	12	20
AE Aur	09.5V	27	11	20
10 Lac	08III	32	14	20
48099	96.5V	49	18	75:
46149	08.5V	51	20	
λ Ori A	08III((f))	52	8	75
S Mon	08III((f))	63	14	90
190864	07III((f))	69	8	100
ι Ori A	08.5III	71	18	140
τ C Ma	09I	75	7	115
193514	07.5III(f)	81	11	120
47432	09.5I	86	14	105
9 Sge	08If	88	13	110
σ Ori	09.5V	89	8	
46223	05((f))	95	11	140
210809	09I	101	13	
δ Ori	09.5I	109	12	140
48279	ON8V	123	22	
190429A	04f	130	5	170
29 C Ma	08.5If	135	9	145
θ^2 Ori A	09V	147	24	165:
175754	08III((f))	161	13	
163892	09III	169	11	
165052	07	172	12	
ξ Per	07.5I	200	10	210
ζ Pup	04ef	208	10	
λ Cep	06ef	214	21	
175876	07	246	27	
192281	05.5(ef)	270	5	290
41161	08V	280	10	300
+60513	07.5	298	12	
13268	07	305	19	
46056	08V(e)	328	23	
217086	06.5	341	8	
ζ Oph	09V(e)	351	18	350
14434	06.5(ef)	400	25	

Star	Spectral Type	V sin i	σ	Slettebak
Spectra traced, but not included in standards				
201345		54	32	
λ Ori B	B0.5V	76	10	75
190429B	09.5III	88	25	
191201		84, 63		
193322	08.5III	94	40	
μ Col	09V	97	20	
θ^1 Ori C	07Vp	98	17	115:
192639	07.5IIIf	103	16	120
34656	07I((f))	106	18	90
15137		106, 178		
14633	ON8.5V	111	50	
46150	05.5((f))	118	25	140
17603	08.5I(f)	119	16	
9 Sgr	04((f))	128	34	140
42088	06.5V	136	13	
53975	07.5V	147	29	
19820	09III	148	20	
216532	09.5V	168	22	
165921		200, 208		
14442	06ef	273	7	
68 Cyg	08V	274	48	
46485	07.5	300	42	
52533	08.5V	307	21	

Slettebak used 10 Lac and HD 57682 as sources of "zero-velocity" profiles.

The O-type standards adopted give very good coverage for all spectral types, and all velocities. Low velocities, from 15 to 150 km s^{-1}, are very well covered, and it is felt that subsequent visual estimates in this regime are accurate to about 20 km s^{-1}—the same as the standards. Although we have an adequate number of standards covering velocities between 150 and 400 km s^{-1}, visually determined velocities in this regime are probably somewhat less accurate. The visual differences in broad, shallow lines are rather subtle, and more difficult to measure precisely.

With a dispersion of 16 Å mm^{-1}, velocities of about 20 km s^{-1} correspond to displacements of 20 μm on the plate. Since this is comparable to the grain size of

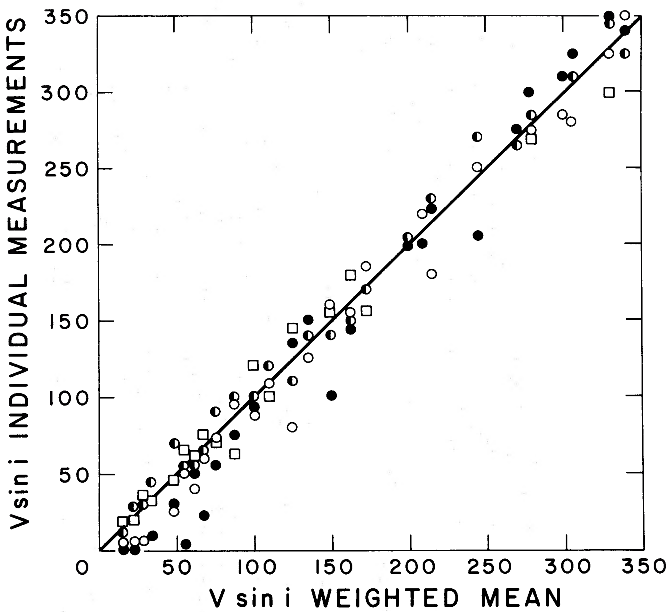

FIG. 2.—Rotational velocity determinations from individual lines plotted against the weighted mean. The measurements from all four lines, Hγ 4340 (○), He I 4388 (□), 4471 (◐), and He II 4541 (●) scatter about the line slope = 1, indicating no systematic errors.

IIa-O, it is felt that the standard deviations less than about 30 km s^{-1} may be attributed to noise in the data. This suspicion is strengthened by inspection of the plates for those stars showing the smallest errors (σ < 10 km s^{-1}). These spectrograms are wider, and their tracings are considerably smoother than those having errors in the 20–30 km s^{-1} range.

For the rest of the O stars, including the southern ones, visual eye estimates of $V \sin i$ were made in the usual fashion by comparison with the standard stars of Table 2. The comparison was made on the Boller and Chivens microcomparator of the Sommers-Bausch Observatory of the University of Colorado. The slight difference in dispersion between the Tololo and Lick spectrograms could readily be accounted for by changing the scale on the comparator. Experiments in repeatability of a derived $V \sin i$ indicated this was not a problem. The adopted values of $V \sin i$ for all 205 stars are listed in Table 3.

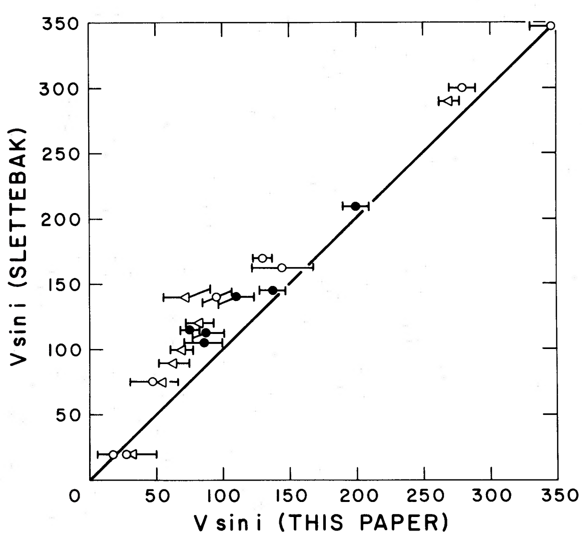

FIG. 3.—Comparison of present rotational velocities with those of Slettebak (1956); the new scale is about 30 km s^{-1} slower than the old one. Main sequence = ○, giants = ▽, supergiants = ●.

IV. ANALYSIS OF THE ROTATIONAL VELOCITIES

The analysis was begun by plotting the data for all O stars as a frequency histogram. The velocity interval was chosen to be 25 km s^{-1}, as this is very nearly the expected accuracy of the measurements. All 205 O-type stars are plotted in Figure 4—both the standards and those determined visually. Double-line spectroscopic binaries were plotted twice if the lines were well enough resolved to measure. A visual inspection of Figure 4 reveals the following features:

1. The distribution is asymmetrical. There are very few stars with velocities less than 50 km s^{-1}, and there is a substantial "tail" to large velocities.
2. There is a maximum in the distribution at about 100 km s^{-1}, a minimum near 200 km s^{-1}, and a smaller secondary maximum near 300 km s^{-1}.

Chandrasekhar and Munch (1950) have indicated a way to analytically find a "best fit" for such a histogram, and to derive a true distribution of rotation velocities from the observed distribution. Essentially, one assumes that the intrinsic rotation velocities of the sample of stars, x, are distributed according to a probability function $f(x)$. The observed projected

Table 3

Rotational Velocities of the O-Type Stars

Star	Spectral Type	V sin i	Star	Spectral Type	V sin i
108	07If	100:	46202	09V	15
1337	09.5III	130	46223	05((f))	95
5005	05.5((f))	95	46485	07.5:*	300
5005C	09V	250	46573	07.5V((f))	95
12323	ON9V	100	46966	08.5V	60
12993	ON6.5V	130	47129	07.5III(f)	75
13268	07:	305	47432	09.5I	86
14434	06.5(ef)	400	15 Mon	08III((f))	63
14442	06ef	273	48099	06.5V	49
14633	ON8.5V	111	48279	ON8V	123
14947	05.5f	130	52266	09.5V	285
15137	09.5III	106, 178	52533	08.5V	307
+60498	09.5V	145	53667	B0.5III	85
+60501	06.5V	200	53975	07.5V	147
15558	05(f)	145	54662	07III	70
15570	04f	130	29 C Ma	08.5If	135
15629	05((f))	130	τ C Ma	09I	75
+60513	07.5:	298	57682	09V	17
16429	09.5I	140	60848	08Ve	162
16691	05f	150	ζ Pup	04ef	208
17505	06(f)	---	68450	09.7Ib*	60
17520	09V	90	69106	05	328
17603	08.5I(f)	119	73882	08.5V*	160
+60586	08III	115	74194	08.5Ib(f)*	170
+60594	09V	330	75211	09Ib*	110
18326	07V	170	75222	09.7Iab*	85
19820	09III	148	75759	09V	50,50
24431	09V	75	76968	09.7Ib*	80
ξ Per	07.5I	200	93028	09V*	60
α Cam	09.5I	85	93128	03V((f))*	130
AE Aur	09.5V	27	93129A	03If*	120
34656	07I((f))	106	93130	06III(f)*	180
35921	09.5:	100	93160	06III((f))*	180
δ Ori	09.5I	109	93204	05V((f))*	130
λ Ori A	08III((f))	53	93205	03V((f))*	150
λ Ori B	B0.5V	76	93206	09Ib	---
36879	07.5III	200	93222	07III((f))*	65
θ^1 Ori C	07Vp	98	93250	03V((f))*	70
θ^2 Ori A	09V	147	-59 2600	06V((f))*	140
ι Ori	08.5III	71	-59 2603	07V((f))*	310
σ Ori	09.5V	89	E303308	03V((f))*	170
ζ Ori	09.5I	110	93403	05III(f)*	270
μ Col	09V	97	93521	09V	400
39680	08Ve	122	93843	05III(f)*	120
41161	08V	280	94963	06.5III(f)*	90
42088	06.5V	136	96670	08p*	150
45314	OBe	---	96917	08.5Ib(f)*	130
46056	08V(e)	328	97166	07.5III((f))*	130
46149	08.5V	51	97253	05.5III(f)*	105
46150	05.5((f))	118	101131	06V*	170

Table 3 (continued)

Star	Spectral Type	V sin i	Star	Spectral Type	V sin i
101190	06V((f))*	120	164438	09III	65
101205	07III((f))*	330	164492	07I	65
101298	06V((f))*	86	9 Sgr	04((f))	128
101413	08V*	140	165052	07:	172
101436	06.5V*	270	165921	07	200,208
105056	09.7Iae*	40	166546	09III	55
112244	08.5Iab(f)*	70	166734	07.5If	150
θ Mus B	09III*	110	16 Sgr	09III	105
114886	09II-III*	270	167659	07I((f))	80
115071	09V	280	167771	07I(f)	80
120678	Ope	350	167971	07.5If	105
124314	06V((f))*	300	168075	06.5III((f))	90:
δ Cir	07.5III((f))*	140	168076	04((f))	111
135591	07.5III((f))*	65	168112	05.5((f))	90
148546	09Ia*	110	168504	08III	100
148937	0.65f	200	169582	05.5(f)	99
μ Nor	09.7Iab*	85	171589	07.5V((f))	91
149404	09Ia*	45	175754	08III((f))	161
ζ Oph	09.5V(e)	351	175876	07:	246
150135	06.5V((f))*	300	+223782	07III((f))	120
150136	05III(f)*	170	186980	08III((f))	70
150958	06.5Iaf*	110	9 Sge	08If	88
151003	09II*	115	188209	09.5I	70
151515	07II(f)*	115	E227018	06.5III	60
151804	08If	50	190429A	04f	130
152003	09.7Iab*	115	190429B	09.5III	88
152147	09.7Ib*	80	190864	07III((f))	69
152218	09.5IV*	130	191201	09III	84,63
152219	09.5III*	250	191612	07.5III(f)	110
152233	06(f)	130	192281	05.5(ef)	270
152246	09III-IV*	280	192639	07.5III(f)	103
152247	09.5II-III	110	193322	08.5III	94
152248	07Ib(f)p*	<100:	193443	09III	110
152249	OC9.5I*	105	193514	07.5III(f)	81
152386	06f	160	195592	09.5I	60
152408	08If	130:	199579	06.5III	110
152424	OC9.5I	85	201345	ON9.5V	54
152623	07V((f))*	120	202124	09.5I	60
152723	06.5III(f)*	130	68 Cyg	08V	274
153919	06f	140	206267	06	---
154368	09.5Iab*	85	207198	09I	70
154811	OC9.7Iab*	110	207538	09.5V	15
155806	07.5IIIe	115	14 Cep	08.5III	120
155889	09IV*	40	19 Cep	09I	75
157857	07:(f)	110	210809	09I	101
159176	07V+07V	170	λ Cep	06ef	214
162978	08.5III((f))	50	10 Lac	08III	32
163758	06.5If*	95	215835	05.5	100
163800	07I((f))	55	216532	09.5V	168
163892	09III	169	216898	09V	80
			217086	07.5:	341
			218915	09.5I	110
			+602522	06.5IIIef	240
			225160	08I(f)	95

*Spectral type due to Walborn
:Luminosity type uncertain

Notes

108	P Cygni profiles
1337	SB2
15137	Double lines partially resolved
17505	Unresolved double lines
19820	SB2
ι Ori	SB2
42088	90 from another plate
45314	Helium lines filled in
46223	109 from another plate
46485	07Vn(e)*
46966	40 from another plate
47129	SB2
15 Mon	same star as S Mon
29 C Ma	SB2
75759	SB2
93205	SB2
93206	Unresolved double lines
93403	SB2
93521	Very broad lines
120678	Sharp displayed λ3889
148937	P Cygni profiles
151804	P Cygni profiles
152218	SB2
152248	Only Hδ, Hγ visible
152249	SB2
152386	P Cygni profiles
152408	P Cygni profiles. Absorption components match ~130 but all lines appear P Cygni
157857	06.5III(f)*
163800	07III((f))*
164492	07.5III((f))*
165052	06.5V((f))*
165921	Double lines
175876	06.5III(f)*
191201	SB2
206267	Unresolved SB2
14 Cep	SB2, both sets of lines seem about equally wide
215835	SB2
217086	07V*

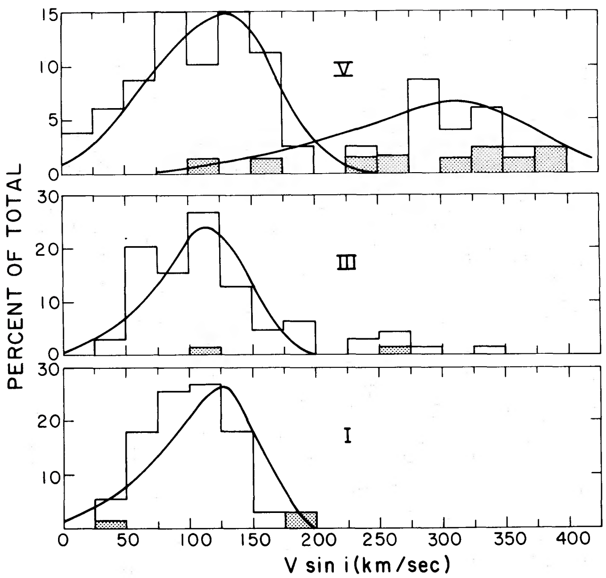

FIG. 4.—Distributions of rotational velocities for main-sequence, giant, and supergiant stars. The Oe and Oef stars are represented by the shaded areas. The shaded supergiant at 40 km s^{-1} is HD 105056 O9.7 Iae (Walborn classification).

velocities $y = x \sin i$ are then distributed according to

$$\phi(y)dy = \int_{i=0}^{\pi/2} \int_{x=0}^{\infty} f(x) \sin i dx di .$$

The distribution of intrinsic velocities is assumed to have the form

$$f(x) = \frac{1}{\sqrt{\pi}} [\exp -(x - x_1)^2 + \exp -(x + x_1)^2] ,$$

in which case

$$\phi(y, x_1) = \frac{y}{\sqrt{\pi}} \int_{y}^{\infty} \frac{\exp -(x - x_1)^2 + \exp -(x + x_2)^2}{x(x^2 - y^3)^{1/2}} dx .$$

As Chandrasekhar and Munch showed, the moments of the observed and intrinsic distributions are related, and those measured moments (the mean and the mean square velocity) allow both $f(x)$ and $\phi(y, x_1)$ to be computed—though not without considerable effort. The procedures suggested by Chandrasekhar and Munch were applied to our data, and the two distributions computed and plotted on the same scale as the histogram.

We first tried computing a single distribution function for the entire set of data. The agreement with the observed distribution was miserable, not matching the histogram well at all. In an effort to improve upon this situation, we considered four factors: the validity of the assumed intrinsic distribution; the influence of other broadening mechanisms; misinterpretation of unresolved binaries; and the possibility of a multiple distribution. The assumed $f(x)$ appears to reproduce very well the observed distributions for B, Be, A, and F0–F2 stars, as shown by Chandrasekhar and Munch (1950) and subsequent workers. There is no obvious reason to expect something different for the O stars. Broadening due to processes like macroturbulence or stellar winds would not explicitly involve the inclination angle. In this case the integrations over i involved in the derivation of $\phi(y, x_1)$ would be inappropriate. We believe that this effect is present, and some insight into its importance was gained in this study. This will be discussed shortly. We traced the spectra of all broad-lined stars and derived velocities from measured profiles. Three stars, HD 165921, HD 191201, and HD 15137, were found to have double lines, but it turned out that the eye estimates of the others had been rather accurate. The revised velocities did not change the observed distribution at all. The crucial realization—which led to the apparent solution to this dilemma—was that trying to fit a single distribution to the entire data set is inappropriate.

Since the minimum near 200 km s^{-1} appears to be real, we divided the data into a "slow" group with $V \sin i < 200$ km s^{-1}, and a "fast" group with $V \sin i \geq 200$ km s^{-1}. The computed distribution functions were found to be in much better agreement with the histograms. The intrinsic distribution for the fast group is very nearly Gaussian, with a peak near 350 km s^{-1} and a $1/e$ full width of 138 km s^{-1}. Perhaps not coincidentally, this is almost exactly the distribution observed for Be stars (Massa 1975).

Additional insight into the nature of the velocity distribution can be gained by plotting to histograms for different luminosity classes separately, as is done in Figure 4. It is seen that the characteristic peak near 100 km s^{-1} is present in all three groups, but the behavior at low and high velocities differs systematically. The main-sequence group shows both the widest range of velocities and the clearest evidence for a bimodal distribution. The Oe stars (Frost and Conti 1976) are generally the most rapidly rotating O types. Among the giants, there are fewer stars at both ends, and only a hint of a bimodal distribution. The supergiants also show few stars at low velocities and none at all faster than 225 km s^{-1}.

One very conspicuous feature in Figure 4 is the failure of the computed functions to reproduce the general shape of the observed distribution. For the giants and supergiants especially, the histogram is skewed, with a steep rise at the low-velocity end and a slower descent toward higher velocities. The fits computed from the moments of the histograms are skewed in the opposite sense, with a more gradual increase and a steeper descent. We feel that the most natural explanation for this discrepancy is that nonrotational "macroturbulent" motions have contributed enough broadening to distort the low-velocity end of the observed distribution.

To demonstrate the plausibility of this hypothesis, the following experiment was performed. We took the observed rotational velocity for the main-sequence stars, and calculated the apparent rotational velocity that would result by a doubling of the radius, and the

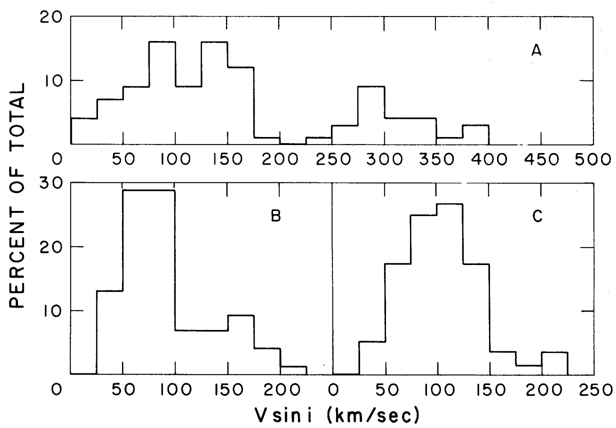

FIG. 5.—A, observed main-sequence distribution; B, distribution calculated from A, assuming doubling of the radius and onset of macroturbulence with characteristic velocity of $V^* = 20$ km s^{-1}; C, observed supergiant distribution.

onset of macroturbulence with a velocity parameter of 20 km s^{-1}. The calculation was performed using the half-width of the He I line 4471 for O9 I. Doubling the radius reduces the rotation velocity by one-half. Turbulence of 20 km s^{-1} produces a half-width about equal to rotation of 30 km s^{-1}. The final half-width is calculated as $w_f = (w_{\rm rot}^2 + w_{\rm tur}^2)^{1/2}$, and the implied rotation velocity is determined from its value. In Figure 5*a*, the observed main-sequence distribution is plotted. The distribution resulting from the above calculation is plotted in Figure 5*b*, and the observed supergiant distribution in Figure 5*c*. The fine details do not (and would not be expected to) agree closely, but the gross features of the observed distribution are reproduced quite well. As anticipated, the turbulence has eliminated the slowest rotators, while expansion has eliminated the fastest ones. The majority of stars are clustered between 50 and 100 km s^{-1}, with the distribution trailing off smoothly to zero at 225 km s^{-1}. Significantly, the turbulence has modified the low-velocity end of the distribution, so that it is now skewed toward higher velocities. This is exactly the feature that the purely rotational functions could not reproduce in Figure 4. Although this is not claimed to be hard proof, it is highly suggestive that the type of mechanism affecting the broadening of supergiant lines is similar to what we propose.

Finally, in Figure 6 the distribution is resolved into both spectral type and luminosity class. The features which stand out in this representation are: (1) the concentration of slowest velocities at later spectral types; (2) the 200 km s^{-1} gap later than type O6; (3) the preponderance of main-sequence stars in the high-velocity group; (4) a possible minimum velocity increasing toward earlier spectral type, and possibly being different for the three luminosity classes; and (5) the absence of rapid rotators of class O3 and O4.

Some plausible interpretation of these features will be discussed in the following section.

V. DISCUSSION

The main-sequence sample represents the youngest stars, whose rotation has been least affected by evolutionary or mass loss effects. This group shows the widest range of velocities, from near zero to a few values in excess of 400 km s^{-1}. This distribution presumably reflects the distribution of angular momentum with which these stars formed. We are somewhat at a loss to understand the apparent existence of a bimodal distribution of rotational velocities for the main-sequence O stars. About one-third of the rapid rotators have been previously identified as Oe stars (Frost and Conti 1976), but not all rapid rotators have yet shown emission lines. It is

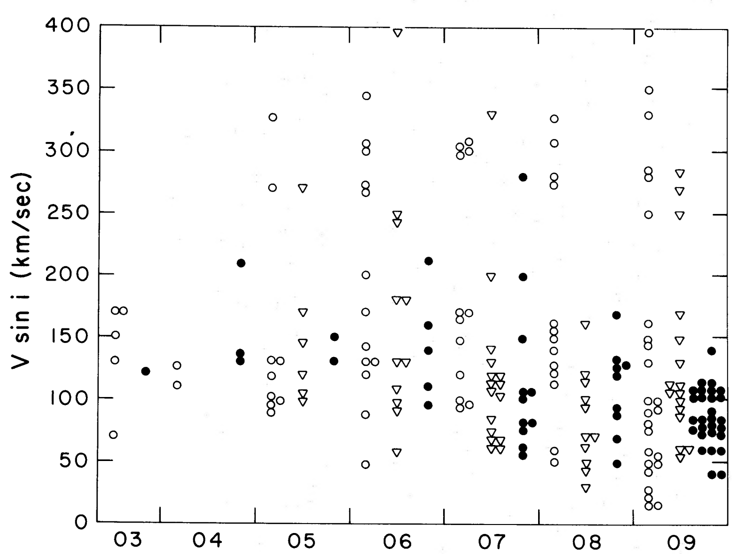

FIG. 6.—Rotational velocities of individual stars plotted as a function of both spectral type and luminosity class; ○ = main sequence (V), V = giants (III), ● = supergiants (I).

quite possible that *all rapidly rotating O stars will show emission at some time*, as might be inferred from the recent shell episode of ζ Oph (Niemelä and Méndez 1974). Possibly a continuation of these events could force a star to lose sufficient angular momentum to move from relatively rapid to slower rotational velocity. However, without differential rotation in the star itself, the angular momentum loss required seems excessive.

As O stars age, the observed broadening would be expected to change, due both to direct evolutionary effects and to possible accompanying changes in the structure of the stars and their atmospheres. We propose a scenario which may help us understand some of the observed characteristics of the distribution of rotational velocities of the evolved O-type stars. The hope is to present a physically plausible mechanism which helps explain the observations while making few ad hoc assumptions.

Evolutionary models (for example, Simpson 1971) predict that, as a massive star evolves, there is a considerable change in the mass distribution within it. Basically, the core contracts, and the envelope expands. The models of Roxburgh (1964) for rotating upper–main-sequence stars indicate that the angular velocity is a monotonically decreasing function of radial distance, and that angular momentum is conserved in spherical shells. If this is the case, as the envelope expands, its equatorial velocity will decrease linearly. Assuming that the observed photosphere before and after expansion occupies roughly the same mass shell, the ratio of final to initial velocities would be the ratio of initial to final radii $V_f/V_i = R_i/R_f$. On this simple basis alone, one expects to see the supergiants rotating more slowly than the main-sequence stars.

It is now widely accepted both observationally (Morton 1967*a*, *b*; Smith 1970) and theoretically (Lucy and Solomon 1970; Castor, Abbott, and Klein 1975), that early-type stars are losing mass at an appreciable rate due to radiation-driven stellar winds. Such mass loss, and its associated angular momentum loss, will also slow the rotation even more as the star ages.

There is one main difficulty with this simple picture that suggests that the physics may be a bit more complicated. We see a few main-sequence stars with fairly sharp lines, indicative of rotational velocities less than 50 km s^{-1}. We would expect to see a greater percentage of evolved stars with sharp lines, since our expectation is that aging stars slow down. However, one quite conspicuous feature of the distributions, seen clearly in Figures 4 and 6, is the absence of sharp-lined supergiants.

At this time it is tempting to consider the possibility of line broadening due to the type of macroturbulence discussed by many authors (see Gray 1976 for a comprehensive discussion). Although quantitative measurement of such turbulence requires higher-quality observational material than that used in this study (Smith 1976), we can make some qualitative remarks about its probable presence. A possible mechanism for driving the turbulence is suggested, after which we indicate those observations that can be more easily understood in terms of such motions.

As the rotating star passes from the core-burning hydrogen phase to the shell-burning hydrogen phase, the luminosity increases, the core contracts, and the envelope expands. As previously noted, angular momentum is conserved in shells, so the core rotates more rapidly but the envelope slows down. This enhances the radial gradient of angular velocity (increases the shear), creating a potentially unstable hydrodynamic situation. The increasing luminosity contributes to the radiative destabilization of the envelope, and eventually the static atmosphere becomes dominated by large-scale turbulence.

When line broadening is treated mathematically as a convolution of an "intrinsic" flux profile with some broadening function, it is found that macroturbulence leads to an observed flux profile that is very similar to a rotationally broadened profile. Moderate resolution and plate noise make the subtle differences difficult to detect observationally (Slettebak 1956). It may be that the absence of slowly rotating supergiants is illusory. Many of them may be rotating quite slowly indeed, but their lines are now broadened mostly by the turbulent velocity field. Turbulent broadening would not, however, affect the rapidly rotating stars as much. A main-sequence star with an equatorial velocity of 300 km s^{-1} would evolve into a supergiant with its photosphere rotating at between 100 and 150 km s^{-1}. The effect of an additional broadening by turbulence would be to increase the width of the profiles only slightly, giving an apparent rotational velocity only about 20 km s^{-1} too high. It therefore seems likely that the absence of very rapidly rotating supergiants is real, and that this circumstance is due entirely to the increased radius.

Another observed feature which may be explained by the presence of turbulence is the apparent minimum velocity seen in Figure 6. This minimum, which seems to be present for all luminosity classes, appears to increase from near 0 km s^{-1} at O9 to perhaps 50 km s^{-1} at O3. It therefore seems plausible to suggest that the narrowest-lined stars of each spectral type are genuinely slow rotators, or are seen pole-on. The residual broadening would then be due to the turbulence—which appears to become more important at higher effective temperatures. This argument is not original; it was proposed by Slettebak (1956), based on a smaller sample of O stars.

There is some evidence that argues against macroturbulence being the dominant cause of the broadening in all cases. In Figure 4 the main-sequence distribution is matched very well, in both form and magnitude, by the derived rotation function. In the derivations of the formulae used to find this function, the rotation problem involves an explicit integration over inclination angles. Turbulence covering the stellar surface would have no such projection effect, and it would seem rather fortunate that a rotation function would fit a histogram of turbulent velocities so well. Furthermore, it would be difficult on hydrodynamic grounds to understand turbulence with characteristic velocities an order of magnitude greater than the sonic velocities in the atmospheres. Also, the addition of a small amount of turbulent broadening, superposed on the rotational broadening, has been shown to change the detailed shape of the distribution in exactly the manner needed to understand the discrepancies for the giants and supergiants in Figure 4.

Our conclusions from this section may be summarized as follows. Early-type stars begin their evolutionary lives on the main sequence with a wide range of angular momentum. This range of angular momentum is reflected in the rotationally broadened spectral lines, from the very sharp and deep lines of HD 46202 and HD 57682 to the diffuse, nearly invisible shallow lines of ζ Oph and HD 14434. The stars evolve off the main sequence with both their radii and luminosities increasing. The increased radius results in a slower photospheric rotational velocity. Differential rotation in the radial direction and increased luminosity destabilize the envelope, resulting in development of large-scale macroturbulence. Among the evolved stars now rotating slowly, macroturbulence is the major broadening agent, producing a minimum width to the lines. The line profiles of rapidly rotating stars are less influenced by turbulence, and more accurately reflect the rotation.

Finally, it will be noticed from Figure 4 that many of the most rapidly rotating O stars have been classified as Oe previously. This strengthens the implication that Oe stars are to O stars as Be stars are to B stars. It will also be noticed that the Oef stars too are rapid rotators, and at least some (e.g., λ Cep and ζ Pup) may be evolved from main-sequence Oe stars.

This research has been supported by the National Science Foundation through grant AST 72-05062 A03. We are grateful to the director of the High Altitude Observatory for giving us access to the microphotometer. We would like to thank referee Dr. A. Slettebak for his useful comments on the manuscript.

REFERENCES

Auer, L., and Mihalas, D. 1972, *Ap. J. Suppl.*, **24**, 193.
Castor, J. I., Abbott, D. C., and Klein, R. I. 1975, *Ap. J.*, **195**, 157.
Chandrasekhar, S., and Munch, G. 1950, *Ap. J.*, **111**, 142.
Conti, P. S. 1973, *Ap. J.*, **179**, 161.
Conti, P. S., and Alschuler, W. R. 1971, *Ap. J.*, **170**, 325 (Paper I).
Conti, P. S., and Leep, E. M. 1974, *Ap. J.*, **193**, 113.
Frost, S. A., and Conti, P. S. 1976, in *IAU Symposium No. 70, Be and Shell Stars*, ed. A. Slettebak (Dordrecht: Reidel), p. 139.
Gray, D. V. 1976, *The Observation and Analysis of Stellar Photospheres* (New York: Wiley).
Lucy, L. B., and Solomon, P. M. 1970, *Ap. J.*, **159**, 879.
Massa, D. 1975, *Pub. A.S.P.*, **87**, 777.
Morton, D. C. 1967*a*, *Ap. J.*, **147**, 1017.
———. 1967*b*, *Ap. J.*, **150**, 535.
Niemelä, V. S., and Méndez, R. H. 1974, *Ap. J.* (*Letters*), **187**, L23.
Rosendahl, J. D. 1970, *Ap. J.*, **159**, 107.
Roxburgh, I. W. 1964, *M.N.R.A.S.*, **128**, 157.
Simpson, E. E. 1971, *Ap. J.*, **165**, 295.
Slettebak, A. 1956, *Ap. J.*, **124**, 173.
Smith, A. M. 1970, *Ap. J.*, **160**, 595.
———. 1976, preprint.
Stoeckley, T. R., and Mihalas, D. 1973, NCAR Technical Note TN/STR-84.
Walborn, N. 1973, *A.J.*, **78**, 1067.

Peter S. Conti and Dennis Ebbets: Joint Institute for Laboratory Astrophysics, University of Colorado, Boulder, CO 80309